Effective Hamiltonians for phosphorene and silicene

Voon, L. C. Lew Yan; Lopez-Bezanilla, A.; Wang, J.; Zhang, Y.; Willatzen, Morten

Published in:
New Journal of Physics

Link to article, DOI:
10.1088/1367-2630/17/2/025004

Publication date:
2015

Document Version
Publisher's PDF, also known as Version of record

Effective Hamiltonians for phosphorene and silicene

2015 New J. Phys. 17 025004

(http://iopscience.iop.org/1367-2630/17/2/025004)

New Journal of Physics
The open access journal at the forefront of physics

Deutsche Physikalische Gesellschaft DPG
IOP Institute of Physics

Published in partnership with: Deutsche Physikalische Gesellschaft and the Institute of Physics

OPEN ACCESS

RECEIVED
1 September 2014

ACCEPTED FOR PUBLICATION
22 December 2014

PUBLISHED
4 February 2015

PAPER

Effective Hamiltonians for phosphorene and silicene

L C Lew Yan Voon[1], **A Lopez-Bezanilla**[2], **J Wang**[3], **Y Zhang**[3] **and M Willatzen**[4]

[1] School of Science and Mathematics, The Citadel, Charleston, SC, USA
[2] Argonne National Laboratory, Lomont, IL, USA
[3] Department of Electrical and Computer Engineering, University of North Carolina, Charlotte, NC, USA
[4] Department of Photonics Engineering, Technical University of Denmark, Lyngby, Denmark

E-mail: llewyanv@citadel.edu

Keywords: silicene, phosphorene, two-dimensional material, k.p, method of invariant, group theory, band structure

Abstract

We derived the effective Hamiltonians for silicene and phosphorene with strain, electric field and magnetic field using the method of invariants. Our paper extends the work of Geissler *et al* 2013 (*New J. Phys.* **15** 085030) on silicene, and Li and Appelbaum 2014 (*Phys. Rev.* B **90**, 115439) on phosphorene. Our Hamiltonians are compared to an equivalent one for graphene. For silicene, the expression for band warping is obtained analytically and found to be of different order than for graphene. We prove that a uniaxial strain does not open a gap, resolving contradictory numerical results in the literature. For phosphorene, it is shown that the bands near the Brillouin zone center only have terms in even powers of the wave vector. We predict that the energies change quadratically in the presence of a perpendicular external electric field but linearly in a perpendicular magnetic field, as opposed to those for silicene which vary linearly in both cases. Preliminary *ab initio* calculations for the intrinsic band structures have been carried out in order to evaluate some of the $k \cdot p$ parameters.

1. Introduction

Graphene is an interesting electronic material because of its two-dimensionality, zero-gap, and linear dispersion near the Fermi energy [1]. These properties differ from standard three-dimensional semiconductors. The study of other two-dimensional materials beyond graphene came about quickly, with BN and MoS_2 being two early choices. More recent candidates include silicene [2] and phosphorene [3], though earlier studies of these two materials exist [4, 5].

Nowadays, much of the study of electronic properties relies on *ab initio* calculations, in particular density-functional theory (DFT). DFT is very powerful in its ability to predict ground-state properties such as structures fairly well. It is less reliable and much more computationally intensive to calculate excited-state properties such as optical and transport properties; the inclusion of an external magnetic field is still a difficult problem and not implemented in standard DFT codes. Empirical tight-binding models have been early alternatives to DFT; indeed, the linear dispersions for both graphene [6] and silicene [2] were first identified using tight-binding models, even though the linear dispersion for silicene was probably first obtained (but not identified) in 1994 using *ab initio* calculations [4].

However, the most versatile and physically-transparent band-structure model is the $k \cdot p$ model [7], often giving energy bands analytically in the vicinity of extrema in terms of meaningful parameters such as effective masses and optical matrix elements. For graphene, this is the Dirac Hamiltonian linear in the wave vector, though nonlinear contributions have also been worked out [8]. For silicene, only the Dirac Hamiltonian, with linear electric field terms, has been written down [9]. For phosphorene, a couple of $k \cdot p$ models have recently appeared [10, 11]. Li and Appelbaum [11], in particular, did a very careful study of the band structure using perturbation theory near the Γ point, identifying the contributions to the effective masses; however, they again did not include external fields.

In the current work, we are therefore concerned with the most general $k \cdot p$ Hamiltonian for silicene and phosphorene, particularly in the presence of external fields since this problem has not been considered fully. We

Table 1. Group of wave vector D_3 at the K point (silicene). k_i are components of the wave vector, ϵ_{ij} of the strain tensor, B_i of an external magnetic field, E_i of an external electric field, and $\mathbf{J}_i$ of an angular momentum operator.

D_3	E	$2C_3$	$3C_2'$	Odd	Even	Matrix
Γ_1	1	1	1		$k_x^2 + k_y^2$, k_z^2, $\epsilon_{xx} + \epsilon_{yy}$, ϵ_{zz}	$\mathbf{1}$
Γ_2	1	1	−1	k_z, B_z	E_z	$\mathbf{J}_z$
Γ_3	2	−1	0	(k_-, k_+), $(B_-, -B_+)$	(E_-, E_+)	$(\mathbf{J}_-, -\mathbf{J}_+)$

Table 2. D_3 multiplication table of irreducible representations.

	Γ_1	Γ_2	Γ_3
Γ_1	Γ_1	Γ_2	Γ_3
Γ_2	Γ_2	Γ_1	Γ_3
Γ_3	Γ_3	Γ_3	$\Gamma_1 \oplus \Gamma_2 \oplus \Gamma_3$

employ the method of invariants to derive such Hamiltonians. The primary goal is to identify possible terms not considered in previous work. A secondary goal is to thus obtain a better understanding of the band structures of silicene and phosphorene.

2. Method of invariants

Here we apply the method of invariants [12] to the materials of interest to us. Since most of the DFT calculations to date have not included relativistic effects and we are considering low atomic number elements, we have left out spin effects in this work; the main consequence in the band structure is the neglect of the small spin–orbit splitting of bands (e.g., for silicene, this is a 1.55 meV splitting at the K point [13]). The symmetries of interest are the space-group symmetries and time-reversal symmetry. Space-group symmetry only requires one to study the character tables of the point-group symmetry, whereas the consideration of time-reversal symmetry requires an application of the Herring test [12]. Details of the theory are not repeated here as we have applied the formalism exactly as presented in [12].

2.1. Silicene

The point of interest for silicene is the K point in the first Brillouin zone (figure 1) since that is where the valence and conduction bands touch with a linear dispersion. In table 1, the group of the wave vector at point K for silicene is shown. We use the expressions

$$k_+ = k_x + ik_y,$$
$$k_- = k_x - ik_y, \tag{1}$$

and similarly for other physical quantities. It can be seen that all the irreducible representations are either one-dimensional or two-dimensional, implying that the energy bands at K are all either non-degenerate or doubly degenerate. The Fermi level is at a point of double degeneracy.

Tables 1–3 allow us to determine the Hamiltonian from combinations of single group functions based on symmetry principles formed. The next step is to apply the Herring test [12]. It follows from the character table of D_3 that

$$\sum_g \chi_i\left(g^2\right) = n, \tag{2}$$

for all representations χ_i, $i = 1, 2, 3$ where $n = 6$ is the order of the group D_3, g is a representation of a group element, and χ is the character of that group element. Further, since a spatial symmetry $\mathcal{R}$ exists such that $-\mathbf{k} = \mathcal{R}\mathbf{k}$ where $\mathbf{k}$ is the K point (and $\mathbf{k} \neq -\mathbf{k}$), all irreducible representations belong to the case $a2$ [12]. In this case, time-reversal symmetry additionally requires all Hamiltonian terms to satisfy

$$\mathcal{T}^{-1}\mathcal{H}\left(\mathcal{R}^{-1}\mathcal{K}\right)\mathcal{T} = \mathcal{H}(\zeta K)^*, \tag{3}$$

where $\mathcal{T}$, $\mathcal{K}$, and $\mathcal{R}$ are the time-reversal operator, a Γ_1 invariant term, and a spatial symmetry operator establishing a link between basis functions at $\mathbf{k}$ and $-\mathbf{k}$, respectively. In the case of silicene, $\mathcal{T} = \mathbf{1}$ and $\mathcal{R} = \mathcal{R}_x$ can be chosen where $\mathcal{R}_x$ denotes reflection in the x axis using a coordinate system where the x axis passes through

Table 3. D_3 coupling constant table ($\Gamma_3 \bigotimes \Gamma_3 = \Gamma_1 \oplus \Gamma_2 \oplus \Gamma_3$). The notations Γ_3^1 and $\Gamma_3^{2'}$ denote the first component of the first Γ_3 function and the second component of the second Γ_3 function, respectively, etc.

$\Gamma_3 \bigotimes \Gamma_3$	
Γ_1:	$\frac{1}{\sqrt{2}}\left(\Gamma_3^1\Gamma_3^{2'} + \Gamma_3^2\Gamma_3^{1'}\right)$
Γ_2:	$\frac{i}{\sqrt{2}}\left(\Gamma_3^1\Gamma_3^{2'} - \Gamma_3^2\Gamma_3^{1'}\right)$
Γ_3^1:	$\Gamma_3^2\Gamma_3^{2'}$
Γ_3^2:	$\Gamma_3^1\Gamma_3^{1'}$

the center of an edge in the honeycomb lattice formed by the silicon atoms (referring to the same choice of coordinate system as in [14]). The symbol ζ takes the value +1 and −1 for even and odd functions under time-reversal symmetry, respectively.

With the preceding analysis, we can write down the most general Hamiltonian for silicene allowed by symmetry. The result is, to leading orders,

$$\mathcal{H} = \mathcal{H}_i + \mathcal{H}_e, \tag{4}$$

$$\mathcal{H}_e = \mathcal{H}^\epsilon + \mathcal{H}^E + \mathcal{H}^B, \tag{5}$$

$$\mathcal{H}_i = a_1\left(k_y\mathbf{J}_x - k_x\mathbf{J}_y\right) + a_2\left(k_x^2 + k_y^2\right) + a_4k_y\left(3k_x^2 - k_y^2\right)\mathbf{J}_z + a_5\left(k_x^2 + k_y^2\right)\left(k_y\mathbf{J}_x - k_x\mathbf{J}_y\right) + \ldots, \tag{6}$$

$$\mathcal{H}^\epsilon = e_1\left(\epsilon_{xx} + \epsilon_{yy}\right) + e_2\epsilon_{zz} + e_3\left(\epsilon_{xx} + \epsilon_{yy}\right)\left(k_y\mathbf{J}_x - k_x\mathbf{J}_y\right) + e_4\Big[\left(\epsilon_{xx} - \epsilon_{yy}\right)k_y + 2\epsilon_{xy}k_x\Big]\mathbf{J}_z + e_5\epsilon_{zz}\left(k_y\mathbf{J}_x - k_x\mathbf{J}_y\right) + \ldots, \tag{7}$$

$$\mathcal{H}^E = c_1E_z\mathbf{J}_z + c_2\left(E_x^2 + E_y^2\right) + c_3E_z^2 + c_4\left(E_xk_y - E_yk_x\right) + c_5\Big[\left(k_x^2 - k_y^2\right)E_x - 2k_xk_yE_y\Big] + c_6\left(E_x^2 + E_y^2\right)\left(k_y\mathbf{J}_x - k_x\mathbf{J}_y\right) + c_8\Big[\left(E_x^2 - E_y^2\right)k_y + 2E_xE_yk_x\Big]\mathbf{J}_z + \ldots, \tag{8}$$

$$\mathcal{H}^B = b_1\left(B_x\mathbf{J}_x + B_y\mathbf{J}_y\right) + b_2B_z\mathbf{J}_z + b_3\left(k_yB_x - k_xB_y\right) + \ldots, \tag{9}$$

where the dots refer to higher-order terms. a_i, b_i, c_i and e_i are $k \cdot p$ parameters which are undetermined in the method of invariants. The H_i terms are intrinsic band-structure Hamiltonians while the other ones exist in the presence of external fields. In the above Hamiltonian, the $\mathbf{J}_i$ matrices represent the pseudospin degree of freedom and are the (2×2) Pauli spin matrices. The difference between the work of Geissler *et al* [9] and the current one is that they were focussed on the interplay between spin–orbit coupling and an external electric field (and, hence, in the topological properties) at the linear level (in k and E_z), whereas we are more interested in understanding the basic band structure of the material beyond the linear terms and in the presence of other external fields. Thus, the a_2 and a_3 terms provide quadratic in k contributions while the a_4 and a_5 are of cubic order but only the a_4 term gives rise to an anisotropic term. Hence, one can readily say that the band structure of silicene to linear and quadratic orders is isotropic and anisotropic effects only manifest themselves if cubic terms become important. A discussion of the band dispersion is provided in the next section.

For comparison, we reproduce the corresponding $\mathcal{H}_i$ for graphene [8]:

$$\mathcal{H}_i = a_{61}\left(k_y\mathbf{J}_x + k_x\mathbf{J}_y\right) + a_{11}\left(k_x^2 + k_y^2\right) + a_{62}\Big[\left(k_y^2 - k_x^2\right)\mathbf{J}_x + 2k_xk_y\mathbf{J}_y\Big]. \tag{10}$$

The sign difference in the a_{61} term is due to a different choice of phase while the a_{62} is the corresponding anisotropy term for graphene. It is seen here to be quadratic in k though it is cubic in k for silicene.

2.2. Phosphorene

Phospherene and its bulk counterpart black phosphorus have the same in-plane translational symmetry and the nonsymmorphic space group is base-centered orthorhombic [11] (figure 2). Its factor group is symmorphic with D_{2h} whose character table and associated functions are shown in table 4.

The multiplication table of irreducible representations for D_{2h} is given in table 5. Note that the parity of the product representation follows the simple rule: $\Gamma_1^+ \bigotimes \Gamma_2^+ = \Gamma_2^+, \Gamma_1^+ \bigotimes \Gamma_2^- = \Gamma_2^-, \Gamma_1^- \bigotimes \Gamma_2^+ = \Gamma_2^-,$

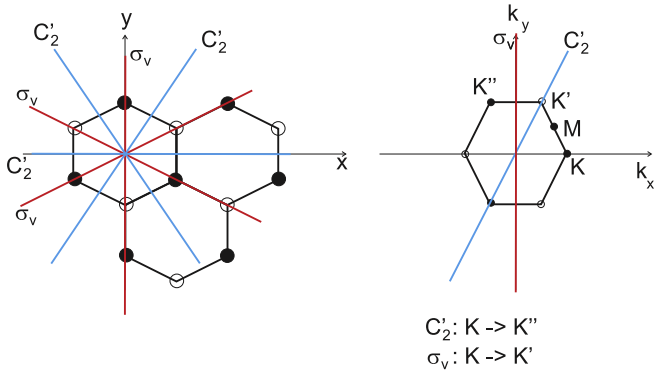

Figure 1. Real (left) and reciprocal (right) space pictures of the structure of silicene. The two atoms (solid and open circles) are at different vertical heights.

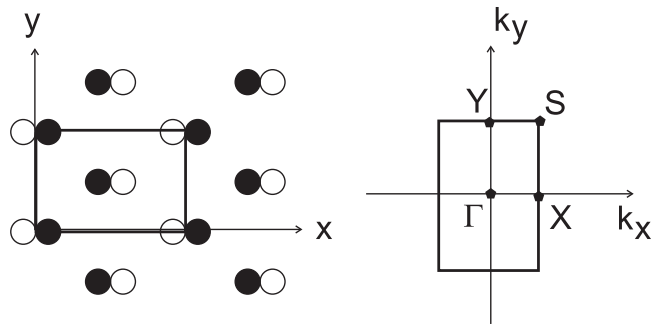

Figure 2. Real (left) and reciprocal (right) space pictures of the structure of phosphorene. The two atoms (solid and open circles) are at different vertical heights.

Table 4. Group of wave vector D_{2h} at the Γ point (phosphorene).

D_{2h}	E	$C_2(z)$	$C_2(y)$	$C_2(x)$	i	σ_{xy}	σ_{xx}	σ_{yz}	Odd	Even	Matrix
Γ_1^+	1	1	1	1	1	1	1	1		k_x^2, k_y^2, k_z^2, ϵ_{xx}, ϵ_{yy}, ϵ_{zz}	**1**
Γ_2^+	1	−1	1	−1	1	−1	1	−1	B_y	$k_x k_z$, ϵ_{xz}	$\mathbf{J}_y$
Γ_3^+	1	1	−1	−1	1	1	−1	−1	B_z	$k_x k_y$, ϵ_{xy}	$\mathbf{J}_z$
Γ_4^+	1	−1	−1	1	1	−1	−1	1	B_x	$k_y k_z$, ϵ_{yz}	$\mathbf{J}_x$
Γ_1^-	1	1	1	1	−1	−1	−1	−1			
Γ_2^-	1	−1	1	−1	−1	+1	−1	1	k_y	E_y	
Γ_3^-	1	1	−1	−1	−1	−1	1	1	k_z	E_z	
Γ_4^-	1	−1	−1	1	−1	1	1	−1	k_x	E_x	

Table 5. D_{2h} multiplication table of irreducible representations.

	Γ_1	Γ_2	Γ_3	Γ_4
Γ_1	Γ_1	Γ_2	Γ_3	Γ_4
Γ_2	Γ_2	Γ_1	Γ_4	Γ_3
Γ_3	Γ_3	Γ_4	Γ_1	Γ_2
Γ_4	Γ_4	Γ_3	Γ_2	Γ_1

$\Gamma_1^- \otimes \Gamma_2^- = \Gamma_2^+$ etc. Since the irreducible representations are all one-dimensional, the coupling constants of product representations are trivial. Further, since $\mathbf{k} = -\mathbf{k} = 0$ at the Γ point and the condition in equation (2) is satisfied by the irreducible representations, all irreducible representations belong to the case $a1$ [12].

We are now in a position to write down the most general Hamiltonian for phosphorene allowed by symmetry. The result is

$$\mathcal{H} = \mathcal{H}_i + \mathcal{H}_e, \tag{11}$$

$$\mathcal{H}_e = \mathcal{H}^\epsilon + \mathcal{H}^E + \mathcal{H}^B + \mathcal{H}^{mix}, \tag{12}$$

$$\mathcal{H}_i = a_1 k_x^2 + a_2 k_y^2 + \sum_{i\leqslant j} a_{ij} k_i^2 k_j^2 + \ldots, \tag{13}$$

$$\begin{aligned}\mathcal{H}^\epsilon = &\left(e_1 + e_2 k_x^2 + e_3 k_y^2\right)\epsilon_{xx} + \left(e_5 + e_6 k_x^2 + e_7 k_y^2\right)\epsilon_{yy} \\ &+ \left(e_9 + e_{10} k_x^2 + e_{11} k_y^2\right)\epsilon_{zz} + \ldots,\end{aligned} \tag{14}$$

$$\begin{aligned}\mathcal{H}^E = &\left(c_4 + c_5 k_x^2 + c_6 k_y^2\right)E_x^2 + \left(c_8 + c_9 k_x^2 + c_{10} k_y^2\right)E_y^2 \\ &+ \left(c_{12} + c_{13} k_x^2 + c_{14} k_y^2\right)E_z^2 + \ldots,\end{aligned} \tag{15}$$

$$\begin{aligned}\mathcal{H}^B = &b_4 k_x B_x + b_5 k_y B_y \\ &+ \left(b_7 + b_8 k_x^2 + b_9 k_y^2\right)B_x^2 + \left(b_{11} + b_{12} k_x^2 + b_{13} k_y^2\right)B_y^2 \\ &+ \left(b_{15} + b_{16} k_x^2 + b_{17} k_y^2\right)B_z^2 + \ldots,\end{aligned} \tag{16}$$

$$\mathcal{H}^{mix} = m_2 B_y E_z k_x + m_3 B_z E_x k_y + \ldots \tag{17}$$

Our intrinsic Hamiltonian agrees with the result of Li and Appelbaum [11].

3. Band structures

We now provide some discussion of the band structures that can be inferred from the Hamiltonians. We are also more interested in revealing the properties analytically than purely numerically using DFT calculations. However, preliminary calculations of the intrinsic band structures have been performed. The DFT-based calculations were conducted using the projector augmented-wave method [15] and the PBE–GGA exchange-correlation functional [16] as implemented in the VASP code [17–19]. The electronic wavefunctions were described using a plane-wave basis set with an energy cutoff of 500 eV for silicene and 1200 eV for phosphorene. Atomic positions were fully relaxed in Γ-centered $25\times25\times1$ for silicene ($9\times9\times1$ for phosphorene) supercells for k-point sampling until residual forces were lower than 5 meV Å^{-1}. For silicene, the lattice constant obtained was 3.867 Å. For phosphorene, the optimized lattice constants were 3.300 and 4.624 Å. In both cases, a large interlayer separation in the z direction was chosen ($\sim$30 Å) to minimize interactions.

3.1. Silicene

We are mainly concerned with the doubly-degenerate Dirac band since the Fermi level crosses it; it is made of p_z and s orbitals from both atoms in the unit cell of silicene [2].

3.1.1. Intrinsic

For an arbitrary direction and keeping terms up to cubic in $\mathbf{k}$, the band structure is given by diagonalizing the H_i Hamiltonian. Writing $k^2 = k_x^2 + k_y^2$, one gets

$$E = a_2 k^2 \pm \sqrt{\left(a_1 + a_5 k^2\right)^2 k^2 + a_4^2 k_y^2 \left(3k_x^2 - k_y^2\right)^2}. \tag{18}$$

Thus, our equation above shows that the intrinsic band dispersion can have quadratic, cubic, … terms in the wave vector.

The a_1 coefficient is related to the Fermi velocity, a_2 is related to an effective mass, a_4 gives rise to anisotropy, and a_5 leads to cubic terms. Along the $K \rightarrow \Gamma$ direction ($k_y = 0$), the band structure simplifies to

$$E(k) = \pm a_1 k + a_2 k^2 \pm a_5 k^3. \tag{19}$$

This reproduces the well-known result for graphene that the Fermi speed is the same for the two bands (figure 3, left). Note that the anisotropy parameter a_4 is absent along this direction.

We have performed a cubic fit of the bands obtained using VASP up to about half-way from K. Rewriting equation (19) as

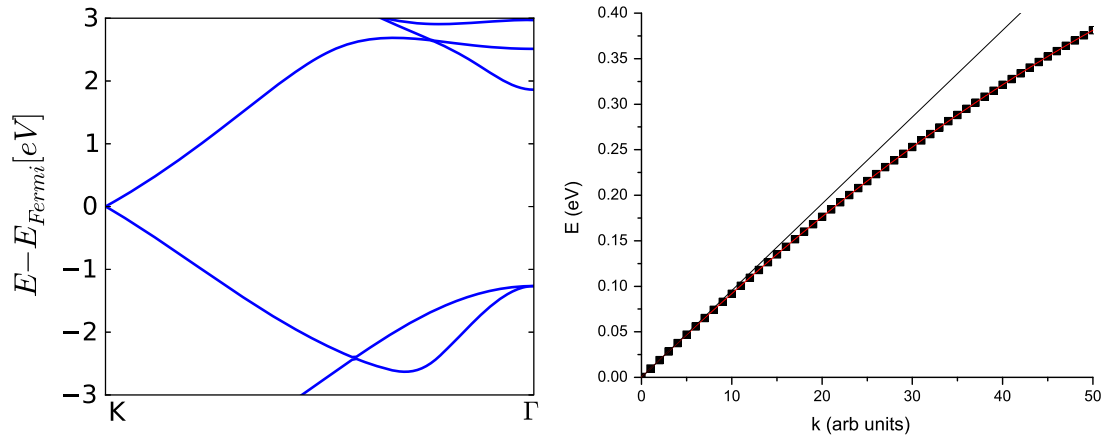

Figure 3. Left: band dispersion for silicene along the K to Γ direction. Right: band dispersion for silicene along the K to $M/2$ direction. The black line is keeping only the linear term.

Table 6. Band fitting for silicene along K to Γ.

	B1	v_F (10^5 m s^{-1})	B2	$m^\star/m_0$	B3	γ (eVÅ^{-3})
VB	−0.040	6.43	-3.461×10^{-4}	−0.66	5.608×10^{-6}	6.65
CB	0.035	5.63	6.315×10^{-4}	0.36	-7.173×10^{-6}	−8.51

$$E(k) = \pm\hbar v_F k + \frac{\hbar^2 k^2}{2m^\star} \pm \gamma k^3, \tag{20}$$

and performing a fit to

$$y(n) = C + (B1)n + (B2)n^2 + (B3)n^3, \tag{21}$$

where n is chosen to be 100 points between K and G, we obtain (with $\Delta k = (2\pi)/(100\sqrt{3}\,a_0)$)

$$v_F = \frac{B1}{\hbar\Delta k} = 4.188 \times 10^6 a_0 B1 \text{ m s}^{-1}, \tag{22}$$

$$m^\star = \frac{\hbar^2\Delta k^2}{2B2} = \frac{2.29 \times 10^{-4}}{B2} m_0, \tag{23}$$

$$\gamma = \frac{B3}{\Delta k^3} = 10^6 \left(\frac{\sqrt{3}\,a_0}{2\pi}\right)^3 B3 = 1.186 \times 10^6 B3 \text{ eVÅ}^{-3}, \tag{24}$$

and where we have used $a_0 = 3.84$ Å.

The results of the curve fitting are given in table 6.

Figure 3 (right) shows the dispersion along $K \to M/2$ (symbols). It can be seen that the linear dispersion (line) is a good approximation only up to about a third of the way.

3.1.2. Strain

In the presence of strain, the Hamiltonian at the K point is given by

$$H_K = e_1\left(\epsilon_{xx} + \epsilon_{yy}\right) + e_2\epsilon_{zz} \equiv \Delta(\epsilon). \tag{25}$$

First, we note that applying strain perpendicular to the plane (ϵ_{zz}) does not change the symmetry at the K point and a zero gap is preserved but there is nevertheless an expected shift in the energy levels. Second, an in-plane uniaxial strain (e.g., ϵ_{xx}), while changing the symmetry, leads to the same energy change for both bands making up the Dirac point since they both have the same deformation potential e_1; thus, the only effect is a shift in energies. Our analysis provides a formal resolution to the controversy from DFT calculations about whether a gap is opened by a uniaxial strain or not [20–23]. Zhao and Mohan *et al* both predicted a gap opening [20, 21]. However, Qin *et al* [24] and Yang *et al* [23] did not obtain a gap and only obtained a shift of the Dirac point. The latter interpreted the disagreement of Zhao to their using insufficient k points near the crossing. However, the influence of strain does significantly change the dispersion at finite $\mathbf{k}$ values, i.e., in the Fermi velocity of those bands.

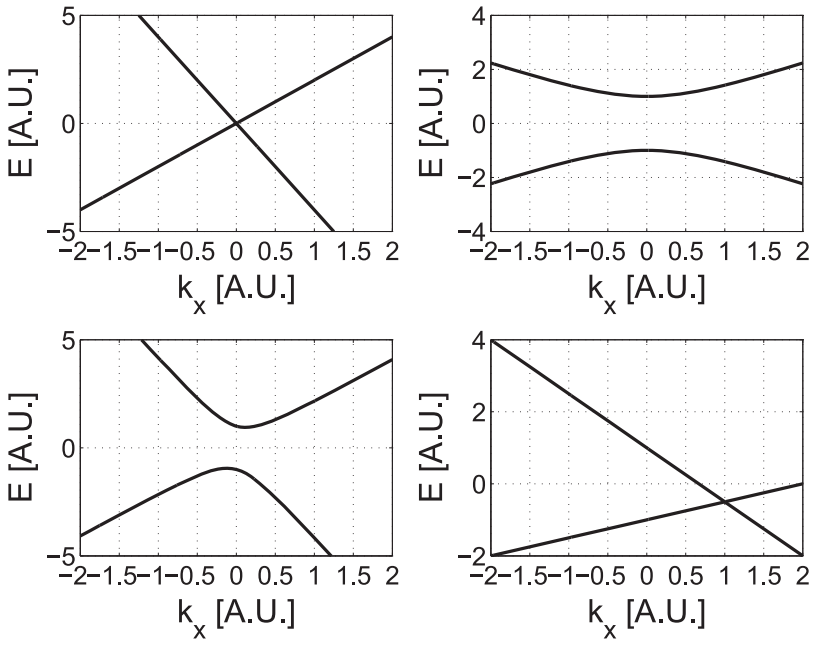

Figure 4. Left: two plots of dispersion relations near the K point for an applied electric field using the expression for $\mathcal{H}^E$ in equation (8) and linear in k. Parameter values are in arbitrary units: (top) $a_1 = 1$, $c_1 = c_4 = 1$, $c_6 = 2$, $E_y = 1$; (bottom) $a_1 = 1$, $c_1 = c_4 = 1$, $c_6 = 2$,, $E_y = E_z = 1$. Right: the same with magnetic field instead: (top) $a_1 = b_1 = 1$, $B_x = 1$; (bottom) $a_1 = b_1 = 1$, $b_3 = 0.5$, $B_y = 1$.

For finite **k** and an arbitrary strain, one can also diagonalize the Hamiltonian to give

$$E(k, \epsilon) = \Delta(\epsilon) \pm \left\{ e_4^2 \left[(\epsilon_{xx} - \epsilon_{yy}) k_y + 2\epsilon_{xy} k_x \right]^2 + \left[e_3 \left(\epsilon_{xx} + \epsilon_{yy} \right) + e_5 \epsilon_{zz} \right]^2 \left(k_x^2 - k_y^2 \right) \right\}^{1/2}. \tag{26}$$

3.1.3. Electric field

In the presence of an electric field, the Hamiltonian at the K point is given by

$$H_K = c_1 E_z \mathbf{J}_z + c_2 \left(E_x^2 + E_y^2 \right) + c_3 E_z^2. \tag{27}$$

An electric field in the z-direction will change the symmetry for silicene (as opposed to graphene which has all the atoms in the plane) and, therefore, a gap will open. Earlier DFT calculations have shown that the gap opening is initially linear in the field (hence $c_1 \neq 0$) and later becomes nonlinear. This behaviour is reproduced by our symmetry analysis. Indeed, by comparing to the DFT calculations of Drummond *et al* [25], one obtains $c_1 = 0.037$ eÅ. No existing calculations allow us to determine c_2 and c_3.

In figure 4 (left), dispersion plots are shown near the K point for an applied electric field $E_y = 1$ (top, in arbitrary units) and for $E_y = E_z = 1$ (bottom, in arbitrary units). Note that the plots are relative energies as they do not include the solution of the equations in the y direction which requires numerically solving the Airy equation.

3.1.4. Magnetic field

Finally, we present the behaviour of the energies in the presence of a magnetic field. First, the Hamiltonian linear in the magnetic field is

$$\mathcal{H}^B = a_1 \left(k_y \mathbf{J}_x - k_x \mathbf{J}_y \right) + b_1 \left(k_y B_x - k_x B_y \right) + b_2 B_z \mathbf{J}_z + b_3 \left(B_x \mathbf{J}_x + B_y \mathbf{J}_y \right). \tag{28}$$

Thus, at the K point, we have

$$H_K = b_2 B_z \mathbf{J}_z + b_3 \left(B_x \mathbf{J}_x + B_y \mathbf{J}_y \right). \tag{29}$$

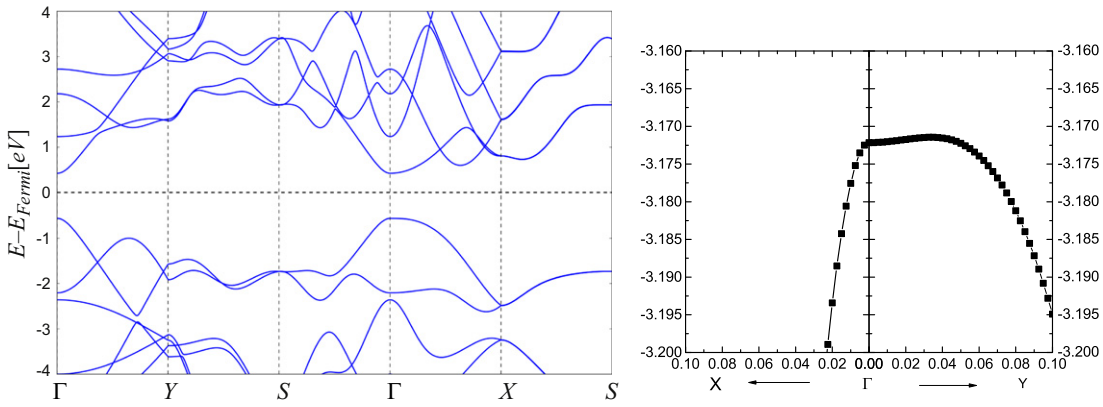

Figure 5. Band structure of phosphorene. On the right is a close up of the highest valence band near the Γ point.

Table 7. Effective masses (in units of m_0) of the highest valence and lowest conduction bands of phosphorene at the Γ point. The effective mass of the VB along ΓY is very sensitive to the computation.

	ΓY	ΓX
CB	1.24	0.173
	1.246 [27], 1.16 [28]	0.146 [27], 0.22 [28]
VB	7.2	−0.160
	3.24 [28]	−0.19 [28]

Similarly to the electric field case, the magnetic-field problem is separable and only the soluble part is plotted in figure 4.

3.2. Phosphorene

For phospherene, since the irreducible representations are all one dimensional, the Hamiltonians are the same as the dispersion relations. Thus, the band structure is simpler to interpret. From equation (13), it can be seen that (in the absence of spin–orbit interaction), only terms in even powers of k_i are allowed. There is also an obvious anisotropy in the effective mass due to the orthorhombic symmetry.

Our DFT calculations (figure 5) are consistent with others already published (e.g., [3, 10]). The gap is almost direct at the Γ point and the GGA value is about 0.98 eV; Tran *et al* [26] have shown that a GW correction increases the gap to 2.0 eV. We performed a fit to our DFT calculations (table 7).

While early calculations reported phosphorene to be a direct-gap semiconductor [3, 5], subsequent calculations have revealed it to be slightly indirect [10, 11, 29] with an almost flat dispersion in the ΓY direction. An interesting observation is the fact that some bands merge along the surface of the Brillouin zone, leading to double degeneracy (even though the character tables of the group of wave vector only reveal one-dimensional irreducible representations). The origin of the band sticking is the nonsymmorphic nature of the space group [30].

3.2.1. Strain

We note that a number of DFT calculations of strained phosphorene have recently been reported [27–29, 31, 32], though all for large strains up to ∼20%. The leading terms in the strain Hamiltonian are

$$\mathcal{H}^{\epsilon} = \left(e_1 + e_2 k_x^2 + e_3 k_y^2\right)\epsilon_{xx} + \left(e_5 + e_6 k_x^2 + e_7 k_y^2\right)\epsilon_{yy} + \left(e_9 + e_{10} k_x^2 + e_{11} k_y^2\right)\epsilon_{zz} + e_{13} k_x k_y \epsilon_{xy}. \quad (30)$$

At the Γ point, the energies are

$$E_i(\epsilon) = E_i + e_1\epsilon_{xx} + e_5\epsilon_{yy} + e_9\epsilon_{zz}, \quad (31)$$

where E_i are the band edges in the absence of strain. Contrary to the case for silicene, now a uniaxial strain in any of the directions or a biaxial strain will change the size of the band gap if the deformation potentials for different bands are different. The particular case of a perpendicular strain has recently been modeled by compressing the

atoms within the unit cell in a DFT calculation and shown to lead to a possible semiconductor-metal transition [10]. Fei *et al* [27] found that a biaxial strain (about 4%) or a zigzag uniaxial strain (between 5 and 6%) can change the order of the lowest two conduction bands.

For a finite wave vector, the total one-dimensional Hamiltonian is

$$\mathcal{H} = E_i(\epsilon) + \left(a_1 + e_2\epsilon_{xx} + e_6\epsilon_{yy} + e_{10}\epsilon_{zz}\right)k_x^2$$

$$\left(a_2 + e_3\epsilon_{xx} + e_7\epsilon_{yy} + e_{11}\epsilon_{zz}\right)k_y^2. \tag{32}$$

3.2.2. Electric field

We note that, in contrast to both graphene and silicene, equation (15) shows that the band energies change quadratically with an externally-applied electric field. At $k = 0$, the band energies for a perpendicular field are

$$E_\Gamma = E_i + c_{12}E_z^2. \tag{33}$$

DFT results just published appear to confirm our prediction [28].

3.2.3. Magnetic field

In an external magnetic field, the one-band problem is exactly solvable in terms of the standard Landau level problem. Thus, with a static magnetic field $\mathbf{B} = (0,\ 0,\ B_z)$ with a vector potential $\mathbf{A} = (0,\ B_z x,\ 0)$, the Hamiltonian is given by [7]

$$H = \frac{p_x^2}{2m_x^*} + \frac{1}{2m_y^*}\left(p_y + eB_z x\right)^2. \tag{34}$$

The eigenfunctions can be separated,

$$f(\mathbf{r}) = \frac{1}{\sqrt{L_y}}e^{ik_y y}\phi(x), \tag{35}$$

and the eigenvalues are equidistant Landau levels

$$E_n = \left(n + \frac{1}{2}\right)\hbar\omega_c, \tag{36}$$

where $\omega_c = eB_z\Big/\sqrt{m_x^* m_y^*}$. Thus, the prediction is that, to the lowest order, a perpendicular magnetic field will change the energy levels linearly.

4. Summary

The method of invariants was used to obtain analytical forms for the Hamiltonians and band structures of silicene and phosphorene beyond the lowest order terms and in the presence of external fields. Differences in the band structures of graphene, silicene and phosphorene are pointed out. Our method provides a formal analysis that is not possible from *ab initio* calculations. Specifically, some of the main conclusions derived from the theory include

- anisotropy in the band structure of silicene shows up at the cubic order whereas they show up at the quadratic level for graphene.
- an in-plane uniaxial strain does not open a gap for silicene.
- a perpendicular strain does not open a gap for silicene but would change the gap for phosphorene.
- to the lowest-order the energies levels of silicene change linearly with an external magnetic field and a perpendicular electric field, whereas, for phosphorene, the energy levels change quadratically with a perpendicular electric field and linearly with a perpendicular magnetic field.

Ab initio calculations for the intrinsic band structures are included and more extensive calculations with external perturbations will be reported in a future publication.

Acknowledgments

LLYV acknowledges the support of the Traubert Chair. Work at Argonne is supported by DOE-BES under contract no. DE-AC02–06CH11357; ALB acknowledges Glue funding from DOE (FWP#70081). MW would like to thank The Citadel for travel support. YZ acknowledges the support of the Bissell Distinguished Professorship.

References

[1] Castro Neto A H, Guinea F, Peres N M R, Novoselov K S and Geim A K 2009 The electronic properties of graphene *Rev. Mod. Phys.* **81** 109
[2] Guzmán-Verri G G and Lew Yan Voon L C 2007 Electronic structure of silicon-based nanostructures *Physical Review* B(Condensed Matter and Materials Physics) **76** 075131
[3] Liu H, Neal A T, Zhu Z, Luo Z, Xu X, Tomnek D and Ye P D 2014 Phosphorene: an unexplored 2D semiconductor with a high hole mobility *ACS Nano* **8** 4033
[4] Takeda K and Shiraishi K 1994 Theoretical possibility of stage corrugation in Si and Ge analogs of graphite *Phys. Rev.* B **50** 14916
[5] Takao Y and Morita A 1981 Electronic structure of black phosphorus: tight binding approach *Physica* **105B** 93
[6] Wallace P R 1947 The band theory of graphite *Phys. Rev.* **71** 622
[7] Lew Yan Voon L C and Willatzen M 2009 *The k · p Method* (Heidelberg: Springer Verlag)
[8] Winkler R and Zülicke U 2010 Invariant expansion for the trigonal band structure of graphene *Phys. Rev.* B **82** 245313
[9] Geissler F, Budich J C and Trauzettel B 2013 Group theoretical and topological analysis of the quantum spin Hall effect in silicene *New J. Phys.* **15** 085030
[10] Rodin A S, Carvalho A and Castro Neto A H 2014 Strain-Induced Gap Modification in Black Phosphorus *Phys. Rev. Lett.* **112** 176801
[11] Li P and Appelbaum I 2014 Electrons and holes in phosphorene *Phys. Rev.* B **90** 115439
[12] Bir G L and Pikus G E 1975 *Symmetry and Strained Induced Effects in Semiconductors* (New York: Wiley)
[13] Liu C-C, Feng W and Yao Y 2011 Quantum spin hall effect in silicene and two-dimensional germanium *Phys. Rev. Lett.* **107** 076802
[14] Koster G F, Dimmock J O, Wheeler R G and Statz H 1963 *Properties of the Thirty-Two Point Groups* (Cambridge: MIT)
[15] Blöchl P E 1994 Projector augmented-wave method *Phys. Rev.* B **50** 17953
[16] Perdew J P, Burke K and Ernzerhof M 1996 Generalized gradient approximation made simple *Phys. Rev. Lett.* **77** 3865
[17] Kresse G and Hafner J 1993 *Ab initio* molecular dynamics for open-shell transition metals *Phys. Rev.* B **48** 13115
[18] Kresse G and Furthmüller J 1996 Efficient iterative schemes for *ab initio* total-energy calculations using a plane-wave basis set *Phys. Rev.* B **54** 11169
[19] Kresse G and Joubert D 1999 From ultrasoft pseudopotentials to the projector augmented-wave method *Phys. Rev.* B **59** 1758
[20] Zhao H 2012 Strain and chirality effects on the mechanical and electronic properties of silicene and silicane under uniaxial tension *Phys. Lett.* A **376** 3546
[21] Mohan B, Kumar A and Ahluwalia P K 2014 Electronic and optical properties of silicene under uni-axial and bi-axial mechanical strains: A first principle study *Physica E: Low-dimensional Systems and Nanostructures* **61** 40
[22] Qin R, Wang C-H, Zhu W and Zhang Y 2012 First-principles calculations of mechanical and electronic properties of silicene under strain *AIP Advances* **2** 022159
[23] Yang C, Yu Z, Lu P, Liu Y, Ye H and Gao T 2014 Phonon instability and ideal strength of silicene under tension *Comput. Mater. Sci.* **95** 420
[24] Qin R, Zhu W, Zhang Y and Deng X 2014 Uniaxial strain-induced mechanical and electronic property modulation of silicene *Nano. Res. Lett.* **9** 521
[25] Drummond N D, Zólyomi V and Fal'ko V I 2012 Electrically tunable band gap in silicene *Phys. Rev.* B **85** 075423
[26] Tran V, Soklaski R, Liang Y and Yang L 2014 Layer-controlled band gap and anisotropic excitons in few-layer black phosphorus *Phys. Rev.* B **89** 235319
[27] Fei R and Yang L 2014 Strain-engineering the anisotropic electrical conductance of few-layer black phosphorus *Nano Letters* **14** 2884 PMID:24779386
[28] Li Y, Yang S and Li J 2014 Modulation of the electronic properties of ultrathin black phosphorus by strain and electrical field *The Journal of Physical Chemistry* C **118** 23970
[29] Peng X, Wei Q and Copple A 2014 Strain-engineered direct-indirect band gap transition and its mechanism in two-dimensional phosphorene *Phys. Rev.* B **90** 085402
[30] Burns G 1977 *Introduction to Group Theory with Applications* (New York: Academic Press)
[31] Hu T, Han Y and Dong J 2014 Mechanical and electronic properties of monolayer and bilayer phosphorene under uniaxial and isotropic strains *Nanotechnology* **25** 455703
[32] Sa B, Li Y, Qi J, Ahuja R and Sun Z 2014 Strain engineering for phosphorene: the potential application as a photocatalyst *The Journal of Physical Chemistry* C **118** 26560